Journal of the Korean Society for Nondestructive Testing
Vol. 28, No. 6 (2008. 12)

Ultrasonic Evaluation of Interfacial Stiffness for Nonlinear Contact Surfaces

Nohyu Kim*†, Hyundong Kim** and Younho Cho***

Abstract This paper proposes an ultrasonic measurement method for measurement of linear interfacial stiffness of contacting surface between two steel plates subjected to nominal compression pressures. Interfacial stiffness was evaluated by using shear waves reflected at contact interface of two identical solid plates. Three consecutive reflection waves from solid-solid surface are captured by pulse-echo method to evaluate the state of contact interface. A non-dimensional parameter defined as the ratio of their peak-to-peak amplitudes are formulated and used to calculate the quantitative stiffness of interface. Mathematical model for 1-D wave propagation across interfaces is developed to formulate the reflection and transmission waves across the interface and to determine the interfacial stiffness. Two identical plates are fabricated and assembled to form contacting surface and to measure interfacial stiffness at different states of contact pressure by means of bolt fastening. It is found from experiment that the amplitude of interfacial stiffness is dependent on the pressure and successfully determined by employing pulse-echo ultrasonic method without measuring through-transmission waves.

Keywords: Interfacial Stiffness, Contact Surface, Contact Nonlinearity, Pulse-Echo Ultrasound

1. Introduction

Contact-type discontinuity such as closed cracks leads to an anomalously high level of nonlinearity. Well-known acoustical manifestation of the nonlinear behavior is the generation of its harmonics. The practical implementation of the second harmonic method has been widely attempted to assess the contact state or to detect cracks in NDE applications. In particular, the transmission and reflection characteristics at contacting surfaces have been the subject of extensive research relating to the evaluation of contact interfaces and integrity monitoring in NDT. The physical nature of the contact acoustic nonlinearity(CAN) has been explained and analyzed by micro-mechanical models for contact-type interface. The variation of contact area due to the deformation of asperities is known to cause the nonlinear elasticity of interfaces. In the previous works, this interface is considered as a nonlinear elastic spring whose stiffness is proportional to the contact area of interfaces (Biwa et al., 2006 and 2007; Delsanto et al., 2002; Kim et al., 2004).

Non-invasive evaluation of the contact condition for solids is also important for the tribology and the design of mechanical components having contacting interfaces (Biwa et al., 2005). Typical examples of the contacting solids found in solid mechanics are fracture surfaces which are often closed and contacting

Received: May 7, 2008, Revised: June 13, 2008, Accepted: June 17, 2008. * Department of Mechatronic Engineering, Korea University of Technology and Education, 307 Gajun-Ri, Byungchun-Myun, Chunan 330-860, Korea ** Graduate School of Mechatronics Engineering, Korea University of Technology and Education, Byungchun-Myun,Chunan 330-860, Korea *** Department of Mechanical Engineering, Pusan National University, Samjun-dong, Keumjun-gu, Pusan 609-735, Korea † Corresponding Author: nykim@kut.ac.kr

under loading. Micro-mechanical behavior of the contacting surfaces is so complicated with nonlinearity that it is hardly understood by micro-scale properties of the solids. Instead those are effectively explained in macro-scale by the interfacial normal and tangential stiffness which are employed to model the nonlinear stress-displacement relation of the contact surfaces as a simple spring-force-displacement system. These interfacial stiffnesses are known to offer useful information on the nature of the contact interface. Ultrasound is an attractive tool for monitoring the contact condition between solid components because of its penetration power and sensitivity to the discontinuity. Therefore, ultrasonic reflection/transmission measurements is considered as one of the most quantitative approaches, yielding interfacial stiffness as a measure of the tightness of contact because the transmission/ reflection spectra of normally incident longitudinal and shear waves are governed by the normal and tangential stiffnesses of the contact interface theoretically(J. Y. Kim et al., 2004 and 2006; Solodov ,1998). Interfacial stiffness may provide not only useful information on the nature of the contact interface, but also the detection tool of a closed crack that hardly produces linear scattering waves.

Interfacial stiffnesses of contacting surfaces have been studied by different principles such as the normal and oblique reflection of bulk waves from interface, the velocity/attenuation of guided waves, and so on. Biwa et al. (2005 and 2006) evaluated the normal stiffness and the tangential stiffness of contacting poly-methyl-methacrylate (PMMA) blocks from both bulk wave reflection and interface wave velocity measurements. However, for the measurement of the interfacial stiffnesses, both of pulse-echo and through-transmission tests are conducted to calculate the reflection and transmission coefficients at the same time. This is often impossible due to difficult access to both sides of the specimen.

In this paper, a new measurement technique is suggested using only one transducer without through-transmission test to generate wave reflection/transmission at the interface. Multiple transmissions and reflections across the interface are produced to estimate interfacial stiffness based on theoretical model for contacting interface. Reflection and transmission coefficients are calculated from consecutive reflected waves from the interface of two contacting plates. A new stress-strain constitutive equation based on a displacement discontinuity analysis is built to simulate the reflection and transmission of a harmonic wave across the contact interface using a simple wave equation. For the demonstration of these characteristics, a solid-solid interface is constructed using steel plates and inspected by 5 MHz shear transducer of 0.5 inch diameter to measure the reflection and transmission waves across the interface at various pressures. The experimental results are discussed to verify the method proposed in this paper.

2. Normal Reflection and Transmission Across Solid-Solid Interface

The reflection and transmission of acoustic waves across contact interface have been investigated and understood well using the classical linear and nonlinear spring model of contact interface. For the linear analysis of reflection/transmission characteristics, solid-solid interface is modeled as a linear spring shown in Fig. 1, which is a simple first-order approximation of general nonlinear stress-displacement relationship used in the classical acoustics of compressed contact interfaces((Biwa et al., 2006 and 2007).

This linear spring in Fig. 1 plays a key role in the pressure-strain relation and constitutive equation of the closed interface, and also contributes to the reflection and transmission of acoustic waves across the interface. Consider a longitudinal plane wave of wave number κ and frequency ω incident to the contact interfaces in z-direction in Fig. 1. Then the incident harmonic

wave $\left(u_z^u(z,t)\right)_i = Ae^{i\kappa(z-ct)}$ from the upper medium generates a reflected wave $\left(u_z^u(z,t)\right)_r = Be^{-i\kappa(z+ct)}$ and a transmitted wave $\left(u_z^u(z,t)\right)_t = Ce^{i\kappa(z-ct)}$ at the interface. The amplitudes of the waves denoted as A, B, and C are a complex magnitude, and the superscripts, u and l, represent the upper and lower medium of the interface, and the subscripts, r and t, mean the reflection and transmission, respectively. Then, the transmission and reflection waves for incident shear wave are given by (N. Kim et al., 2008),

$$(u_z^l(z,t))_t = \frac{2(\frac{\kappa_x}{Z})}{2(\frac{\kappa_x}{Z})+i\omega} Ae^{i\kappa(z-ct)} \quad (1)$$

$$(u_z^u(z,t))_r = -\frac{i\omega}{2(\frac{\kappa_x}{Z})+i\omega} Ae^{-i\kappa(z+ct)} \quad (2)$$

where, $Z=\rho c$ is the acoustic impedance, c is the wave velocity, and κ_x is the interfacial stiffness. Therefore, the reflection and transmission coefficients, R and T, at contact interface are simply given in terms of interfacial stiffness κ_x by (N. Kim et al., 2008),

$$R=\frac{1}{\sqrt{1+4(\frac{\kappa_x}{Z\omega})^2}},\ phase\ \phi_R=\tan^{-1}(2(\frac{\kappa_x}{Z\omega})) \quad (3)$$

$$T=\frac{2(\frac{\kappa_x}{Z\omega})}{\sqrt{1+4(\frac{\kappa_x}{Z\omega})^2}},\ phase\ \phi_T=\tan^{-1}(-\frac{1}{2(\frac{\kappa_x}{Z\omega})}) \quad (4)$$

Eqns. (3) and (4) show that reflection and transmission coefficients are a function of interfacial stiffness κ_x, acoustic impedance(Z), and frequency(ω), so that the stiffness is calculated inversely from the value of reflection or transmission coefficient, i.e., R or T.

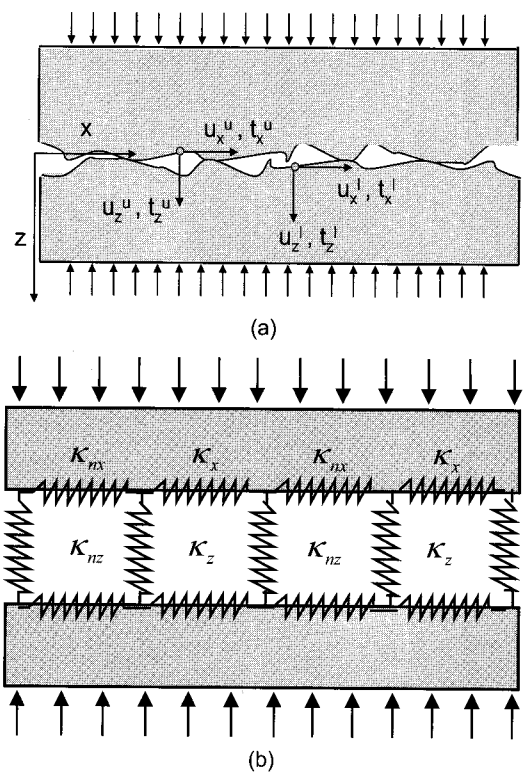

Fig. 1 Mathematical model of contact interface, (a) physical cross-section, (b) linear spring model

3. Measurement of Reflection and Transmission Coefficients

Reflection and transmission coefficients of plane waves in eqns.(3) and (4) can be determined under three assumptions. First assumption is that the coefficients are independent of propagation direction. It means that they have the same values whether acoustic waves travel downward or upward in Fig. 1. This is reasonable if two contacting surfaces have the same micromechanical property, i.e., the same profile of microscopic asperity in statistical senses. Second assumption is that there are no hysteresis and nonlinearity during interaction with acoustic wave at any condition of contacting pressure. Lastly it is supposed that contact condition between acoustic transducer and specimen is maintained as same as possible throughout the whole experiment, so that the variation from contacting pressure of transducer is negligible. Then, when a normal incident wave u_i is applied to solid-solid contact interface of two identical plates as shown in Fig. 2(a), the first

three reflection waves from the plates may be represented in Fig. 2(a) as L_1, L_2, and L_3 in order. L_1 is the first arriving wave reflected once directly from the interface between the plates, while L_2 and L_3 are reflected waves traveling two times and three-times of the distance the wave L_1 does. Therefore, the round-trip distance of L_1 is the thickness of the plate, 2d, that of L_2 is 4d, and L_3 6d. While L_1 is composed of only one reflection wave u_r as shown in Fig 2(a), L_2 and L_3 have two and three reflection wave components. L_2 is the sum of two kinds of waves, which are $u'_{r1}+u'_{r2}$. L_3 is $u''_{r1}+u''_{r2}+u''_{r3}$. One example of these consecutive waves obtained from experiment is represented in Fig. 2(b). In

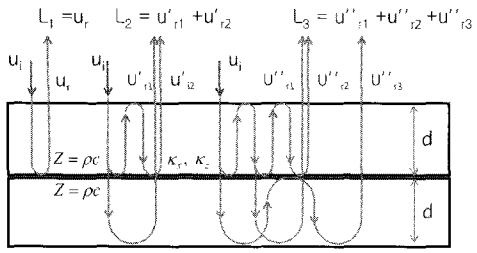

(a)

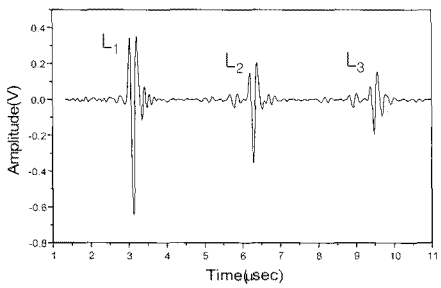

(b)

Fig. 2 Multiple reflection waves. (a) acoustic waves in contacting plates, (b) waveforms of L_1, L_2, and L_3

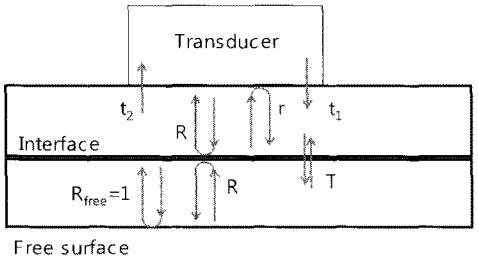

Fig. 3 Reflection and transmission coefficients in contacting plates

order to detect these waves, an acoustic transducer mounted on the specimen of Fig. 2(a) is shown schematically in Fig. 3.

Suppose that an plane harmonic wave, $u_i = Ae^{i\omega t}$, is applied to the interface of reflection and transmission coefficients, R and T in Fig. 3. If all transmission and reflection coefficients between the transducer and plates are given by r, t_1, and t_2 as represented in Fig. 3, then the waves L_1, L_2, and L_3 incident to the transducer are expressed under the assumptions mentioned earlier by followings.

$$L_1 = u_r = Re^{i(\phi_R)} \cdot t_1 \cdot t_2 \cdot e^{i(\phi_t)} e^{-\alpha d} \cdot Ae^{i\omega t}$$

$$L_2 = u'_{r1} + u'_{r2} = [T^2 \cdot t_1 \cdot t_2 \cdot e^{i(2\phi_T + \pi)} + rR^2 \cdot t_1 \cdot t_2 \cdot e^{i(2\phi_R + \phi_t)}] \cdot t_1 \cdot t_2 \cdot e^{i(\phi_t)} e^{-\alpha 2d} Ae^{i\omega t}$$

$$L_3 = u''_{r1} + u''_{r2} + u''_{r3} = [RT^2 e^{i(2\phi_T + \phi_R + 2\pi)} + 2rRT^2 e^{i(2\phi_T + \phi_R + \phi_r + \pi)} + r^2 R^3 e^{i(3\phi_R + 2\phi_t)}] \cdot t_1 \cdot t_2 \cdot e^{i(\phi_t)} e^{-\alpha 3d} Ae^{i\omega t} \quad (5)$$

In eqn. (5), ϕ_R, ϕ_T, and ϕ_r are the phase shift of the waves asscociated with the corresponding reflections and transmissions R, r, T. ϕ_t is total phase angle shift during transmission processes represented by t_1 and t_2 in Fig. 3. α is the attenuation coefficient of the waves in the plates. With phase relations and energy conservation at the interfaces between the transducer(PZT) and specimen(steel), eqn. (5) reduces to,

$$When\ Z_{PZT} < Z_{Specimen(steel)},\ \phi_r = \pi \text{ and } \phi_T = \phi_R - \frac{\pi}{2}$$

$$Energy\ conservation: R^2 + T^2 = 1$$

$$L_1 = R \cdot t_1 \cdot t_2 \cdot Ae^{i(\phi_R + \phi_t + \omega t)} e^{-\alpha d}$$

$$L_2 = [T^2 - rR^2] \cdot t_1 \cdot t_2 \cdot Ae^{i(2\phi_R + \phi_t + \omega t)} e^{-\alpha 2d}$$

$$L_3 = [-RT^2 - 2rRT^2 + r^2 R^3] \cdot t_1 \cdot t_2 \cdot Ae^{i(3\phi_R + \phi_t + \omega t)} e^{-\alpha 3d} \quad (6)$$

From eqns. (5) and (6), L_2 and L_3 are simplified in terms of the magnitude and the phase of the wave L_1 such that,

$$\frac{|L_2|}{|L_1|}=\frac{|T^2-rR^2|e^{-\alpha d}}{R}=\frac{1}{R}|T^2-rR^2|e^{-\alpha d}$$
$$\frac{|L_3|}{|L_1|}=|-T^2-2rT^2+r^2R^2|e^{-\alpha 2d} \quad (7)$$

By eliminating the attenuation effect in eqn. (7), the following non-dimensional parameter may be introduced.

$$\frac{|L_3|}{|L_1|}\Big/\left(\frac{|L_2|}{|L_1|}\right)^2=\frac{R^2|-T^2-2rT^2+r^2R^2|}{|T^2-rR^2|^2}=\frac{R^2|R^2(r+1)^2-(2r+1)|}{|R^2(r+1)-1|^2} \quad (8)$$

Eqn. (8) shows that the reflection and transmission coefficients, R and T, at contact interfaces are simply obtained only if the reflection coefficient r is measured or guessed. In the case that the value r is not known or hard to determine, Eqn. (7) could be used to calculate the reflection or transmission coefficient by measuring the attenuation coeffcient α of the plates. It can be measured more accurately and easily in experiment than the reflection coefficient r.

4. Experiment and Results

In order to demonstrate qualitatively the validity of the model proposed in this paper, a solid-solid interface is created artificially by putting together two steel plates with high-tension bolts. Before joining two plates, they are ground flat well and smooth enough to guarantee area-contact instead of line-contact. Surface roughness of two plates was less than 10 μm in peak-to-peak $R_{\max}$. The plate specimen has a hexagonal washer-shape of 50 mm in outer diameter and 25 mm in inner diameter with 10 mm thickness. A jig to hold ultrasonic transducer on the specimen and to apply compression pressure on the specimen at the same time is also made and mounted on the top surface of the steel plates by using bolt and nut as shown in Fig. 4(b).

Two hexagonal washer-type plates were initially put together by tightening the bolt-nut with hands, so that only a small amount of pressure is imposed on the interface of the plates. At this negligible pressure, shear ultrasonic wave was sent on the top of the specimen to the interface. Then reflected waves L_1, L_2, and L_3 from the interface are selected and saved for analysis and measurement of interfacial stiffness. In experiment, for convenience of calculation, L_2 and L_3 are all normalized by L_1 and inserted into eqn. (8) to obtain reflection coefficient R first. The value of r on the right side of eqn. (8) was set 0.16, which is the theoretical reflection coefficient between PZT and steel.

The specimen is tightened by torque wrench so as to apply compression load to the interface. The torque is increased from zero up to 75 kg.m by 10 kg.m. At each load, the specimen with

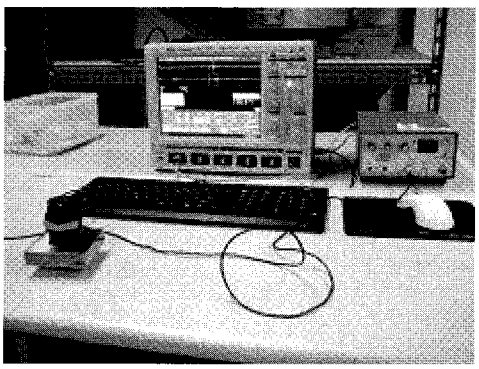

(a)

(b)

Fig. 4 Measurement of interfacial stiffness for contact solids, (a) experimental configuration, (b) test specimen

contact interface is examined at the same position by pulse-echo tests to measure the reflection and transmission energy across the crack using pulse shear wave (5 MHz). The variations of the amplitudes of the first three consecutive reflection signals are detected, one of which is presented in Fig. 5. Waves in Fig. 5 are the normalized waveforms of L_2 , that is, $\frac{L_2}{|L_1|_{\max}}$ obtained by dividing the amplitude of L_2 by the maximum of L_1. Similarly, $\frac{L_3}{|L_1|_{\max}}$ is also calculated and combined with the results in Fig. 5 to determine R (or T). These R and T values are again put into eqn. (3) or (4), which gives interfacial stiffness at the load condition. Experimental results for the measurement of interfacial stiffness at different levels of pressure are summarized in Table 1, where reflection/ transmission coefficients are listed with interfacial stiffness. It is observed that the interfacial stiffness increases very much with the compression load and indicates a severe nonlinearity. This nonlinear characteristic is represented again by graph in Fig. 6, where the interfacial stiffness

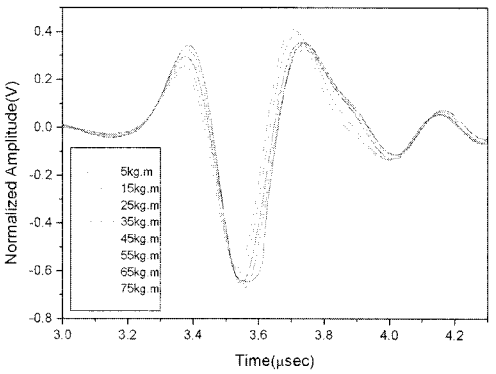

Fig. 5 Variation of the wave L_2 by the increase of tightening torque for the specimen

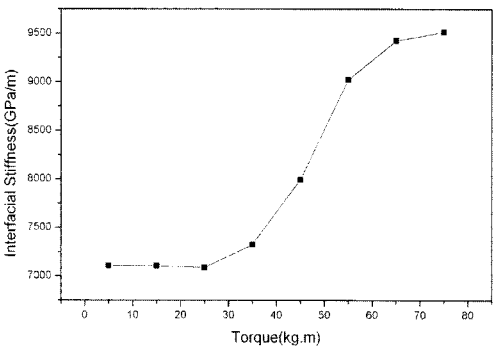

Fig. 6 Variation of interfacial stiffness with the increase of tightening torque for the specimen

Table 1 Measurement results

Torque	Amplitude		Reflection Coefficient(R)	Transmission Coefficient(T)	Stiffness Coeff. (K_z ,GPa/m)	Material Impedance
0 kg.m	|L2/L1|	0.807	0.9878	0.0243	2882.8	
	|L3/L1|	0.554				
5kg.m	|L2/L1|	0.562	0.9323	0.1308	7103.9	
	|L3/L1|	0.348				
15kg.m	|L2/L1|	0.480	0.9323	0.1307	7103.9	Z_{PZT}=18 (MRayl)
	|L3/L1|	0.254				
25kg.m	|L2/L1|	0.409	0.9326	0.1303	7086.4	Z_{Steel}=25 (MRayl)
	|L3/L1|	0.181				
35kg.m	|L2/L1|	0.347	0.9285	0.1378	7323.2	
	|L3/L1|	0.169				
45kg.m	|L2/L1|	0.270	0.9165	0.1601	7992.5	ρ_{PZT}=7.5 (g/cm^3)
	|L3/L1|	0.199				
55kg.m	|L2/L1|	0.228	0.8970	0.1953	9023.6	
	|L3/L1|	0.362				ρ_{Steel}=7.8 (g/cm^3)
65kg.m	|L2/L1|	0.215	0.8892	0.2093	9421.7	
	|L3/L1|	0.474				
75kg.m	|L2/L1|	0.227	0.8874	0.2126	9512.6	
	|L3/L1|	0.581				

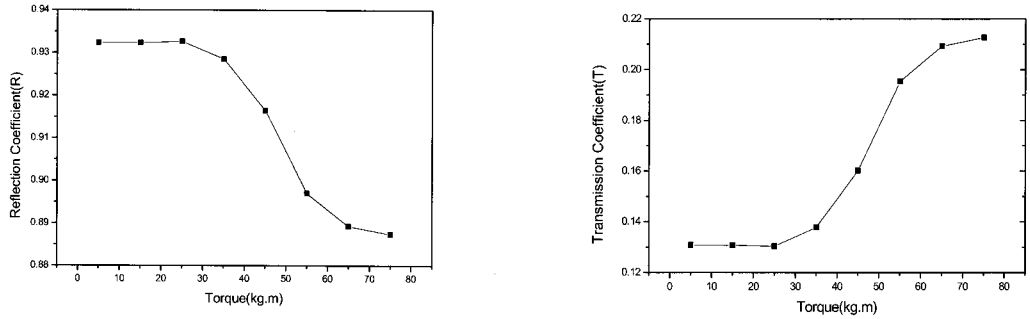

(a) (b)

Fig. 7 Variation of reflection/transmission coefficients with the increase of tightening torque, (a) reflection Coefficient, (b) transmission coefficient

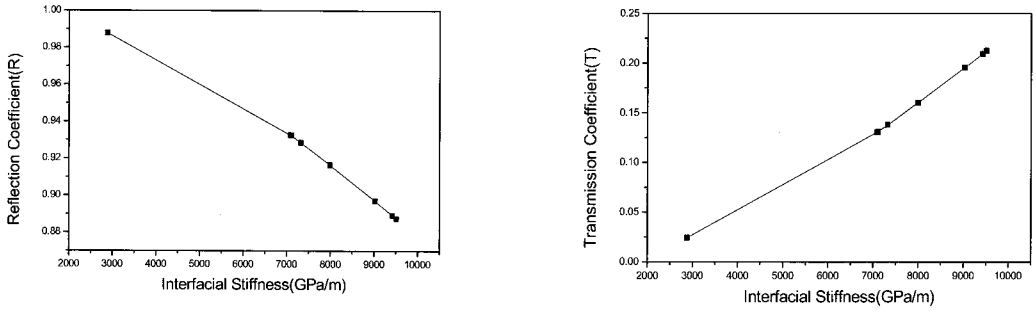

(a) (b)

Fig. 8 Relation of reflection/transmission coefficients to interfacial stiffness, (a) reflection coefficient, (b) transmission coefficient

is calculated from eqns. (3) and (4). Reflection and transmission coefficients obtained from eqn. (8) are displayed again in Fig. 7. Finally the relationship between reflection/transmission characteristics and interfacial stiffness is plotted in Fig. 8, where a clear correlation can be seen. It is concluded from experimental results that interfacial stiffness is an excellent parameter that could tell contact state of solid-solid interface such as closed cracks and bonded joints. As interfacial stiffness goes to zero, reflection coefficient of interface becomes unity, which means that two contacting solids come apart. Conversely, if interfacial stiffness becomes very large, two contacting solids bond together tightly.

5. Conclusions

An ultrasonic method for the measurement of interfacial stiffness in solid-solid contact interface is proposed using pulse-echo signals without through-transmission signals. Mathematical derivation and formulation are made to determine interfacial stiffness based on reflection and transmission coefficients of the interfaces. Three consecutive echo signals in amplitude are captured in experiment and analyzed to calculate the coefficients R and T, by which the stiffness value is obtained without special phase measurement or advanced signal processing. For the demonstration of these characteristics of the hysteretic model, a simple contacting interface was made by joining two identical steel plates with bolt and examined by pulse-echo tests to measure the reflected waves from the contact interface. It was found from the study that the interfacial stiffness is highly dependent on the pressure exerted on the interface. Experimental results showed that the interfacial stiffness increased with the pressure (torque value applied

to the specimen) as expected in theory. The more pressure is applied to the interface, the more transmission but the less reflection across the interface occurs. It is concluded that the interfacial stiffness determined from the pulse-echo method developed in this paper may serves as a tool for the characterization of nonlinear contact interfaces both in quantitative and qualitative sense.

Acknowledgments

This work was supported by the Korea Science and Engineering Foundation (KOSEF) of Korean government (MEST).

References

Biwa, S., Hiraiwa, S. and Matsumoto, E. (2006) Experimental and Theoretical Study of Harmonic Generation at Contacting Interface, *Ultrasonics*, Vol. 44, pp. 1319-1322

Biwa, S., Hiraiwa, S. and Matsumoto, E. (2007) Stiffness Evaluation of Contacting Surfaces by Bulk and Interface Waves, *Ultrasonics*, Vol. 47, pp. 123-129

Biwa, S., Suzuki, A. and Ohno, N. (2005) Evaluation of Interface Wave Velocity, Reflection Coefficients and Interfacial Stiffnesses of Contacting Surfaces, *Ultrasonics*, Vol. 43, pp. 495-502

Kim, J. Y., Baltazar, A. and Rokhlin, S. I. (2004) Ultrasonic Assessment of Rough Surface Contact between Solids from Elasto-Plastic Loading-Unloading Hysteresis Cycle, *J. of the Mech. & Phy. of Solids,* Vol. 52, pp. 1911-1934

Kim, J. Y., Baltazar, A. J., Hu, W. and Rokhlin, S. I. (2006) Hysteretic Linear and Nonlinear Acoustic Responses from Pressed Interfaces, *International Journal of Solids and Structures*, Vol. 43, pp. 6436-6452

Kim, N. and et al. Reflection and Transmission of Acoustic Waves across Nonlinear Contact Interface, *Journal of the Korean Society for Nondestructive Testing*, Vol. 28, No. 3, pp. 292-301(2008)

Solodov, I. Y. (1998) Ultrasonics of Non-Linear Contacts: Propagation, Reflection, and NDE Applications, *Ultrasonics*, Vol. 36, pp. 383-390